Chalcogenide Letters Vol. 7, No. 6, June 2010, p. 413-422

INFLUENCE OF ZINC ON OPTICAL, ELECTRICAL AND STRUCTURAL PROPERTIES OF (Zn_xCd_{1-x})S FILMS

D. GHONEIM
Faculty of Science, Physics Department, Al-Azhar University (Girls), Cairo, Egypt

$Zn_xCd_{1-x}S$ thin films have been prepared in the entire composition range from CdS to ZnS on glass substrate using the solution growth technique. To deposit good quality films, optimum conditions have been determined. Wide band gap ternary films have many applications in heterojunction solar cells. The optical, electrical resistivity and structure of these films have been studied by optical transmission, conductivity technique, scanning electron microscopy (SEM) and X-Ray diffraction (XRD). It was noticed that the microstructure and lattice parameter and the values of the absorption edge shifted towards the shorter wavelength region and hence the direct band gap energy varied from 2.47 ev for CdS to 3.5 ev for ZnS films. Electrical conductivity studies revealed that the resistivity increased with the increase of Zn content.

(Received May 29, 2010; accepted June 25, 2010)

Keywords: Zn-Cd-S, thin films, electrical, optical properties, SEM, XRD

1. Introduction

Recently there is tremendous interest on the nanoscale semiconductor particles and thin films, due to novel properties generated from quantum confinement effect. The quantum confinement effect changes the physical and chemical properties of the materials [1].

Semiconductor nanoparticles have a number of applications; specifically II-VI compound semiconductors (CdS, ZnS, CdSe). Nanomaterials have an immense potential in photovoltaic applications [2-4] and as a luminescent materials [5-7]. Among these, CdS is an n-type direct band gap (2.4ev) semiconductor material and is widely used as a window layer for $CuInSe_2$, CdTe based solar cells [8]. Efficiencies of these solar cells are not too high due to the mismatching of lattice parameters and also of band gap. By introducing Zn into CdS materials, $Zn_xCd_{1-x}S$ alloy semiconductors is formed and its band gap lies between 2.4 ev (CdS) and 3.6 ev (ZnS) at room temperature in the bulk sate. The band gap energy of the ternary alloy semiconductors could be tuned in the range of binary semiconductors band gap. Hence for a better possibility of increasing the efficiency of a solar cell, tunable band gap material like $Zn_xCd_{1-x}S$ or $Zn_xCd_{1-x}Se$ are required. $Zn_xCd_{1-x}Se$ ternary compound is also potentially useful as a window material for the fabrication of p-n junctions without lattice mismatch in the device based on quarternary materials like $CuIn_xCa_{1-x}Se_2$[9], $CuIn(s_xSe_{1-x})_2$ etc. [10]. There are a number of reports on the properties of $Zn_xCd_{1-x}S$ films [11-18] prepared by various techniques such as molecular beam epitaxy (MBE) [19], chemical vapor deposition [20], spray pyrolisis [21], screen printing [22], sol-get [23,24], simultaneous evaporation [25-27], true liquid crystalline templating [28], and solution grown (SGT) [11-17,29,30]. The (SGT) appears to be a relatively simple and inexpensive method to prepare a homogenous film with controlled composition.

In this paper, $Zn_xCd_{1-x}S$ thin films were prepared using (SGT). The optical, electrical, and structural properties of these compounds were investigated as a function of Zn content.

2. Experimental

Thin films of $Zn_xCd_{1-x}S$ with varying composition x=0.0,0.1, 0.3, 0.5, 0.7, 0.9, 1) have been grown on glass substrates by growth technique [11-17,29,30]. The different compositions were obtained by controlling the reaction time period, temperature, and pH $\sim$ 11-4 of the solution

[29]. In the process of fabrication of the heterojunction the $Zn_xCd_{1-x}S$ layer grown on $Zn_xCd_{1-x}S$ thin film was deposited onto glass substrates.

The structure of the films were studied by X-ray diffraction patterns using CuK_α line (λ = 1.5405Å) and scanning electron microscopy (SEM) which measured the grain size of the films. The optical transmission measurements were carried out at room temperature using a double-beam spectrophotometer (Shimadzu model UV-160A) in the spectral range from 300 to 700 nm. The four-probe test was used to measure the resistivity of $Zn_xCd_{1-x}S$ thin films.

3. Results and discussion

3.1. Optical characteristics

Fig. 1 shows spectral behavior transmission T at normal incidence of light in the wavelength (300-700 nm) of the $Zn_xCd_{1-x}S$ films. It was noticed that the transmittance decreases as Zn content decreases and the values of the absorption edge shift toward shorter wavelengths with increasing Zn content. These results are in agreement with literature data [18, 22]. The direct allowed optical band gap Eg is estimated from the plots of $(\alpha\ \lambda v)^2$ versus (λv). The values of band gap were changed from 2.47ev (CdS sample) to 3.54 ev (Zn sample). The effective shift in the band gap by 1.07 ev is significant in the present work. The band gap values increased due to the increase x (Zn content) as shown in Table 1. Table 1 also shows the values of energy gap Eg(ev), wavelengths at absorption edge, and error ratio. The dependence of the band gap on the CdS content is shown in Fig. 2. It is clear from the figure that the band gap increases with decreasing Cd content which agrees with Bonn *et al.,* result [31].

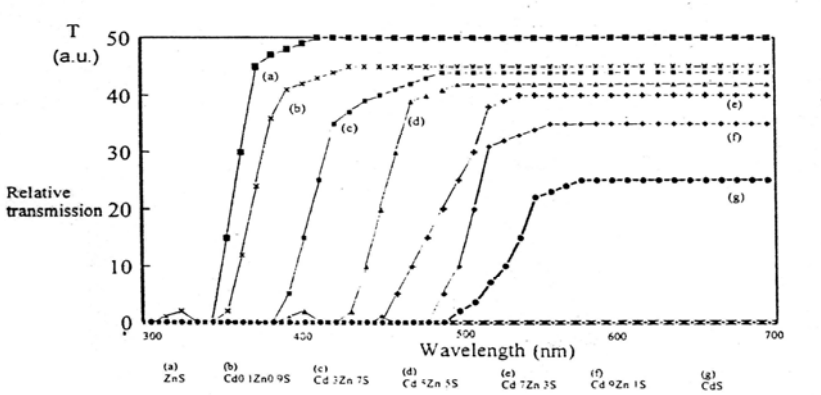

Fig. 1. The optical transmittance T vs wavelength λ of $Zn_xCd_{1-x}S$ thin films for different vales of x.

Table 1. Comparison of band gap energy (Eg), wavelengths and error ratio of $Zn_xCd_{1-x}S$ films

Composition	λ(nm)	E_g (eV)	Error ratio
Cds	502.7	2.47	0.088
$Zn_{0.1}Cd_{0.9}S$	484	2.56	0.01
$Zn_{0.3}Cd_{0.7}S$	450	2.76	0.129
$Zn_{0.5}Cd_{0.5}S$	433.25	2.86	0.07
$Zn_{0.7}Cd_{0.3}S$	383	3.24	0.097
$Zn_{0.9}Cd_{0.1}S$	353.3	3.51	0.12
ZnS	343.3	3.54	0.064

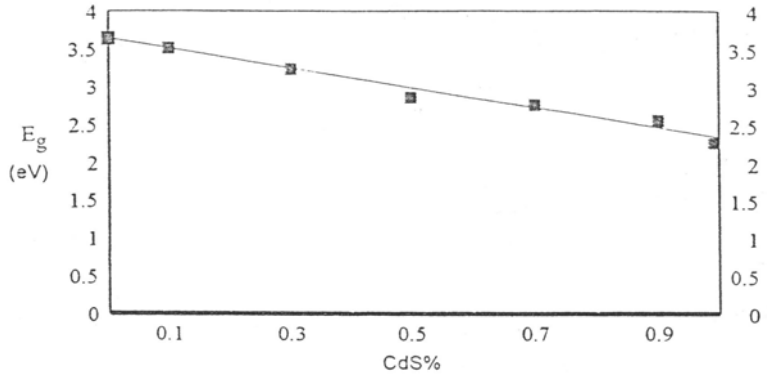

Fig. 2. The relation between the band gap Eg and CdS contents.

The variation of Eg with x can be calculated from the following quadratic equation:

$$Eg(x) = Eg(o) + 0.7x + 0.5x^2 \quad (1)$$

Where Eg(o) is the band gap energy of CdS. The variation of Eg with x is linear as shown in Fig. 3 and in well agreement with results [11]. Kwok *et al.* [16] reported similar empirical formula for $Zn_xCd_{1-x}S$ microcrystalline material.

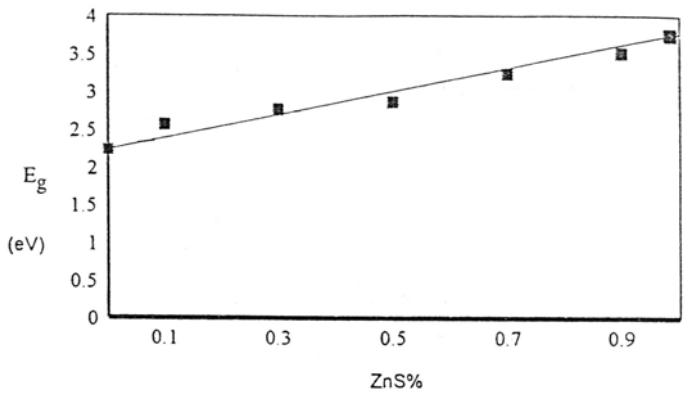

Fig.3. The variation of optical band gap of $Zn_xCd_{1-x}S$ thin films on x (Zn contents).

3.2. Electrical conductivity

Table (2) illustrates the values of resistivity (ρΩcm) by using four-probe test, and thicknesses of $Zn_xCd_{1-x}S$ films which is determined by using weight difference. From Table (2) we observed that the thicknesses of the films decreases as Zn content increases, while the resistivity increases as Cd content decreases. Fig. 4 and 5 show the relation between thicknesses , log resistivity and ZnS content. The experimental data is in agreement with [11]. N-Sugama *et al.* [32], K. Park *et al.* [22] and G. Padam *et al.* [11] explained that the increase in resistivity and small thicknesses of these films with increasing Zn concentration is attributed to the film nature (porosity, texture) in addition to the decrease in the grain size of the films which were prepared by solution growth technique.

Table 2. Comparison of resistivity ρ, log ρ and thicknesses of $Zn_xCd_{1-x}S$ films.

Composition	t(°A)	Resistivity ρ (Ωcm)	log ρ (Ω.cm)
Cds	3209.39±1163.23	$3.0858x10^{9}$	9.489±0.4805
$Zn_{0.1}Cd_{0.9}S$	3553.25±166.524	$5.1959\ x10^{9}$	9.716±0.9359
$Zn_{0.3}Cd_{0.7}S$	2974.57±537.61	$1.5409\ x10^{11}$	11.1878±1.261
$Zn_{0.5}Cd_{0.5}S$	1969.2±13.01	$4.843\ x10^{10}$	10.685±0.563
$Zn_{0.7}Cd_{0.3}S$	1798±228.999	$8.87\ x10^{13}$	13.948±0.555
$Zn_{0.9}Cd_{0.1}S$	907.57±387.32	$4.466\ x10^{14}$	14.6499±0.224
ZnS	463.17±211.12	$6.1365\ x10^{14}$	14.788±0.358

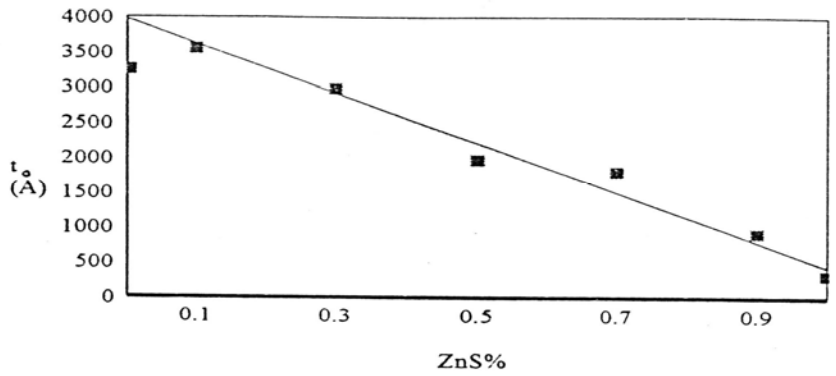

Fig. 4. The variation of thicknesses of $Zn_xCd_{1-x}S$ thin films on x (Zn contents).

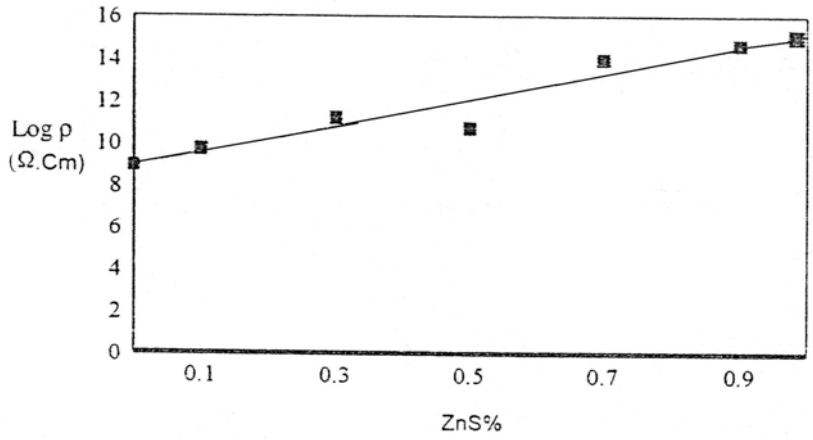

Fig. 5. The relation between the logarithmic resistivity ρ and ZnS contents.

3.3. Structure properties

Scanning electron microscopy (SEM) type (TEOL 5400) was used to determine the grain size of $Zn_xCd_{1-x}S$ films grown on glass substrate. Fig. 6 shows the surface morphology of uniform deposition of CdS film which shows texture shape with holes [17]. Besides, Fig. 7A through 7G show that the increase in Zn content leads to the disappearance of holes with appearance of some grains which make grains in film to appear as nest to texture film. We noticed that the best homogenous film is at composition x = 0.5.

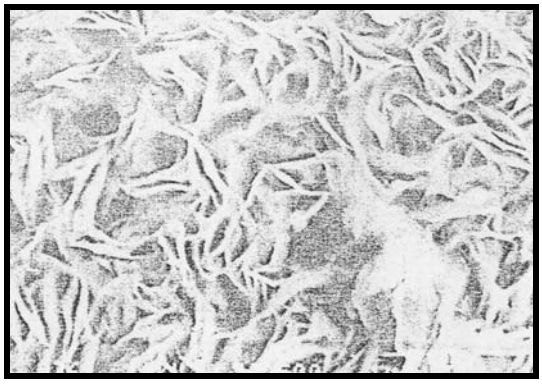

Fig. 6. SEM micrograph of Cds thin film

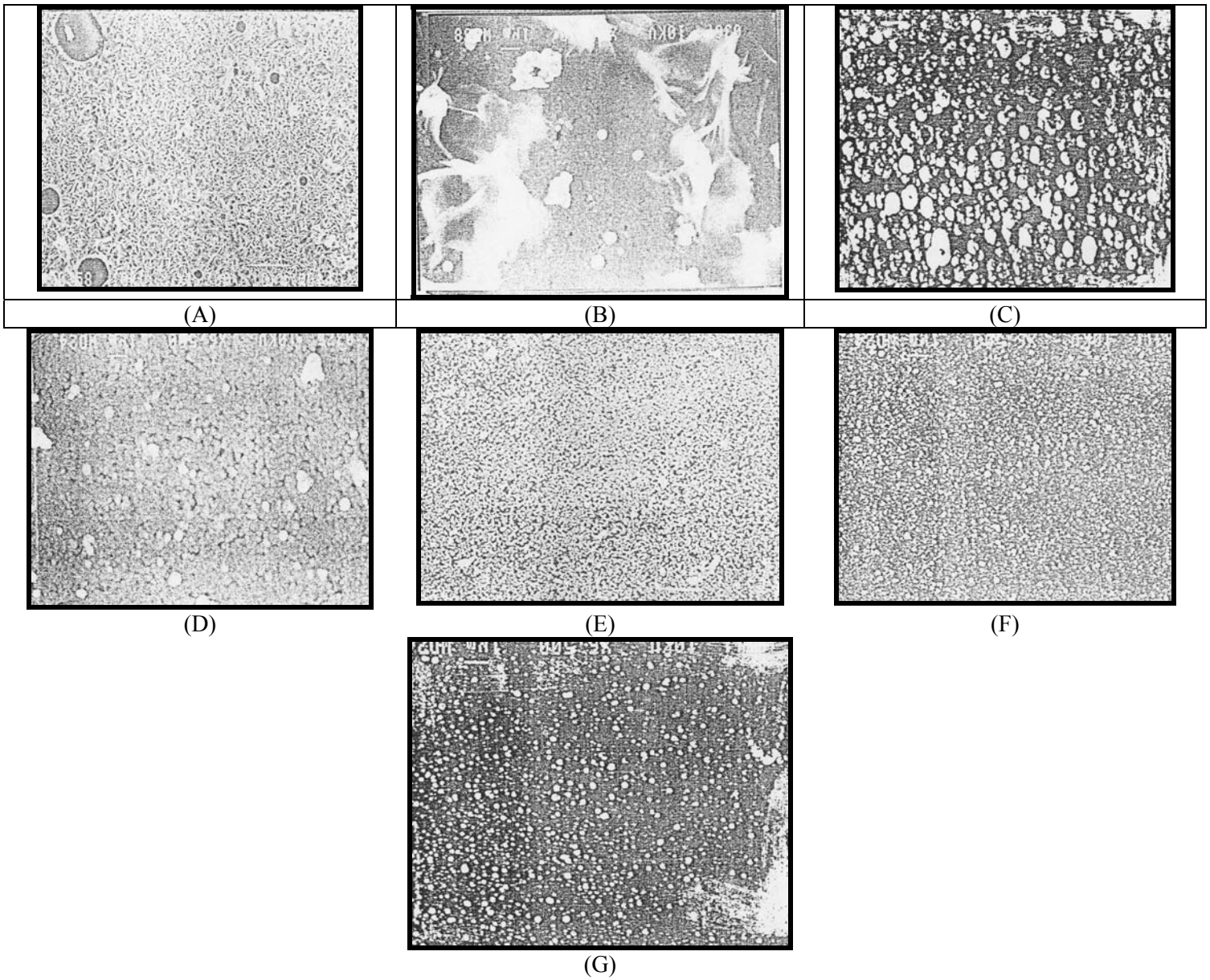

Fig. 7. SEM micrograph of $Zn_xCd_{1-x}S$ thin films (A) CdS, (B) $Zn_{0.1}Cd_{0.9}S$, (C)$Zn_{0.3}Cd_{0.7}S$, (D)$Zn_{0.5}Cd_{0.5}S$, (E)$Zn_{0.7}Cd_{0.3}S$, (F)$Zn_{0.9}Cd_{0.1}S$ and (G) ZnS

Table (3) shows the values of the grain size of $Zn_xCd_{1-x}S$ films. It's clear that the largest value of grain size CdS film (≃ 0.50 967μm). Fig. 8 shows the grain size vs. Zn content. The grain size decreases as Zn content increases which agrees with data [11, 32-34].

Table 3. The grain size of the $Zn_xCd_{1-x}S$ thin films.

Composition	Cds	$Zn_{0.1}Cd_{0.9}S$	$Zn_{0.3}Cd_{0.7}S$	$Zn_{0.5}Cd_{0.5}S$	$Zn_{0.7}Cd_{0.3}S$	$Zn_{0.9}Cd_{0.1}S$	ZnS
Grain size $x = \bar{x} \pm \left(2.776x \frac{S}{\sqrt{n}} \right)$ (μm)	-	0.50967 ± 0.0738	0.47704 ± 0.0299	0.3885 ± 0.0526	0.34733 ± 0.0549	0.26229 ± 0.0517	0.16148 ± 0.01456

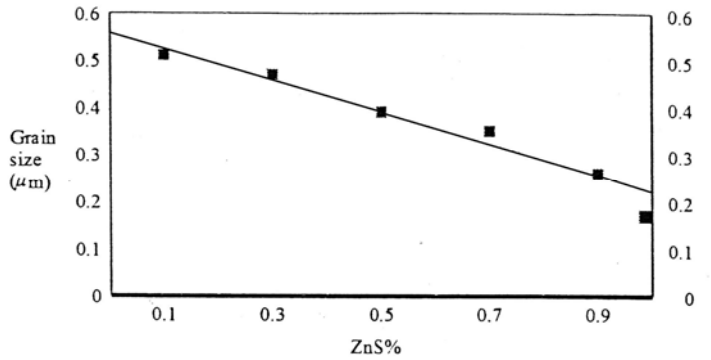

Fig. 8. The variation of grain size of $Zn_xCd_{1-x}S$ thin films on x(Zn contents)

Information about the structure of these $Zn_xCd_{1-x}S$ films are obtained from X-ray diffraction patterns (XRD) technique. Fig. 9 shows diffraction of deposited films of composition X=0.0. The diffraction spectra of Fig. 9 were obtained by scanning 2θ in the range of 24-52 and CdS film shows a single diffraction peak at 2θ = 26.5°. This peak could be associated with the (002) reflection of the hexagonal modification or the (111) reflection of the cubic modification [35]. Fig. 10 (a and b) shows the X-ray diffraction (XRD) pattern of $Zn_xCd_{1-x}S$ films for different values of x=0.0, 0.1, 0.3, 0.7 and 0.5.

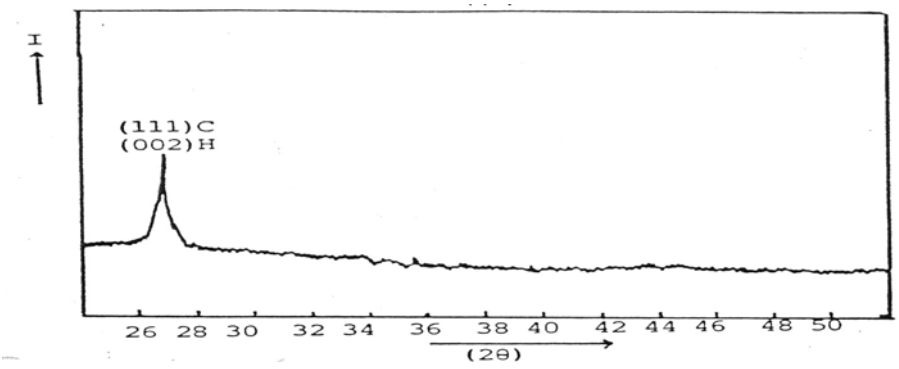

Fig. 9. X-ray diffraction pattern for CdS

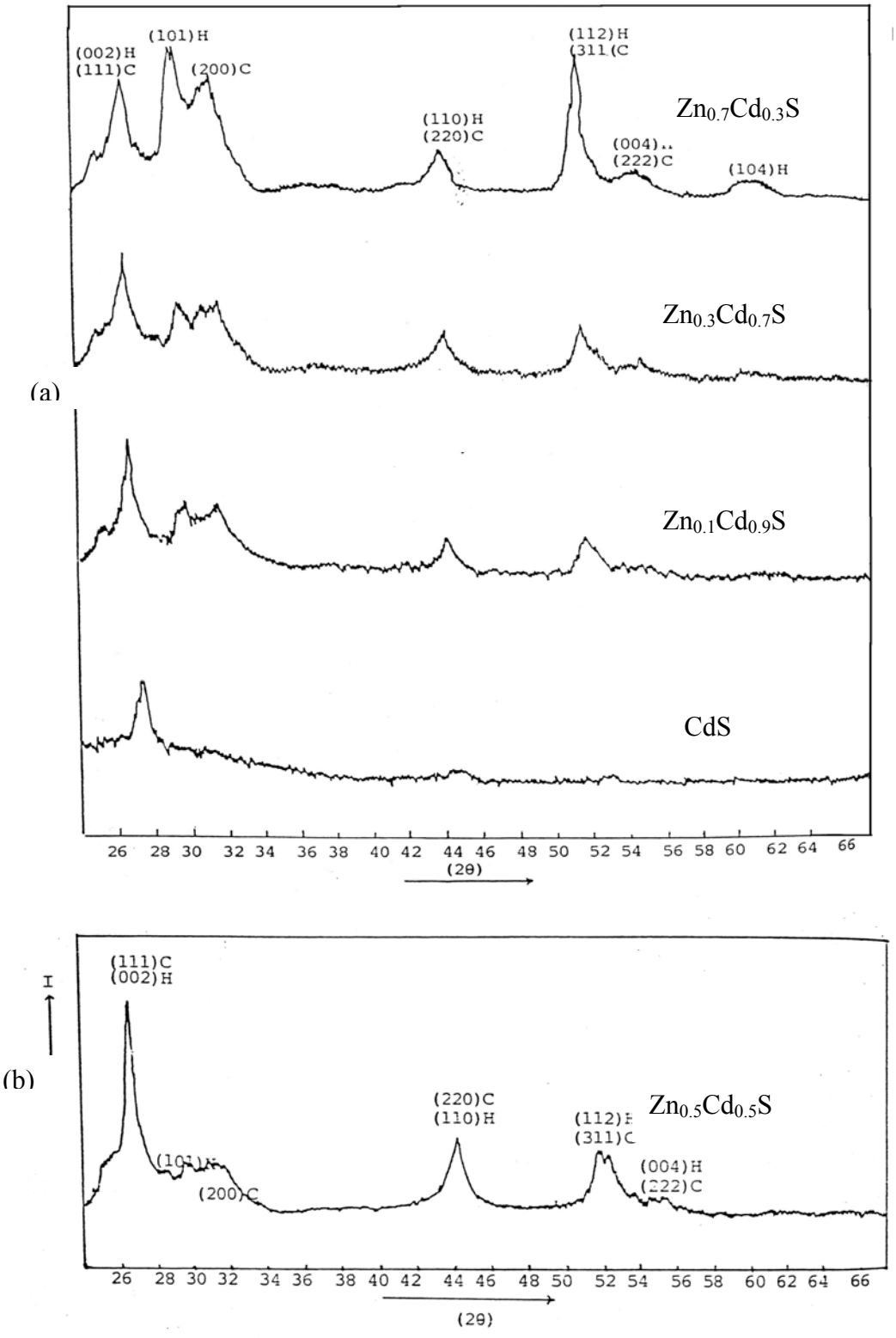

Fig. 10. (a) X-Ray diffraction pattern for $Zn_xCd_{1-x}S$ thin films (b) X-Ray diffraction pattern for $Zn_{0.5}Cd_{0.5}S$ thin film.

Table (4) gives representative data for the estimated values of lattice constants a, c and the volume of the unit cell V after comparison with ASTM card. The predominant case which appears

from Table (4) shows that the structure exhibits a mixture of both cubic and hexagonal phases [22,33,35].

Table 4. The lattice constant of $Zn_xCd_{1-x}S$ thin films.

Composition	Hexagond			Cubic	
	a(°A)	c(°A)	V(°A)	a(°A)	V(°A)
Cds	4.077375	6.6851	96.25	5.786496	193.75
$Zn_{0.1}Cd_{0.9}S$	4.074835	6.68254	96.09	5.7691994	192.02
$Zn_{0.3}Cd_{0.7}S$	4.0648	6.6270	94.83	5.75216375	190.32
$Zn_{0.5}Cd_{0.5}S$	4.08497	6.669375	96.38	5.7712196	192.22
$Zn_{0.7}Cd_{0.3}S$	4.0524434	6.514431	92.65	5.696588917	184.86
$Zn_{0.9}Cd_{0.1}S$	4.01206	6.41652	89.45	5.6160	177.13
ZnS	-	-	-	-	-

The variation of lattice parameter a and c with the x (Zn content) is shown in Fig. 11(a ,b and c) which shows nearly linear plot [11,18]. A gradual decrease in lattice parameter a and c are observed as Zn composition (x) increases. This trend is consistent with Vegard's law and indicates a homogenous alloy structure [18]. Fig. 12 a and b represents the variation of V unit cell volume of $Zn_xCd_{1-x}S$ with composition x which is linear, and decreases as Zn content increases.

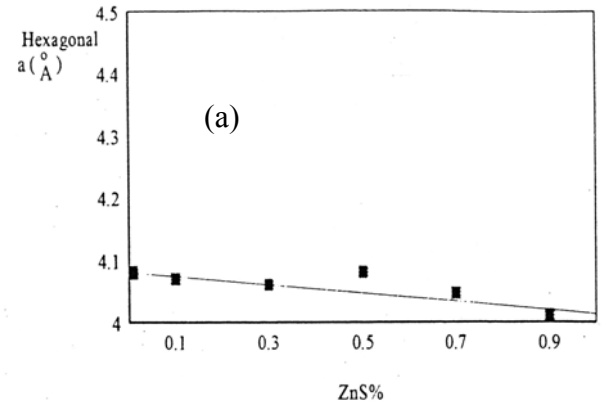

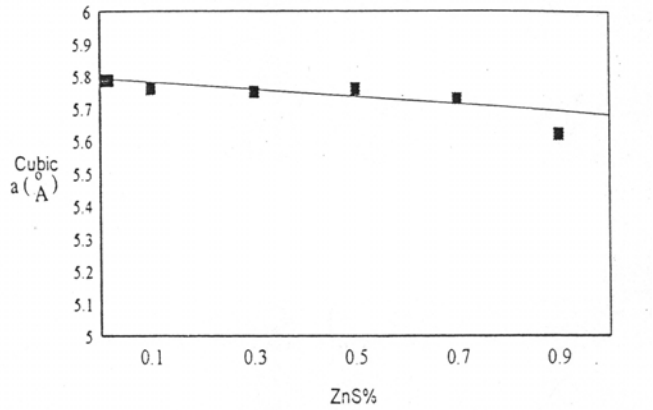

(b)

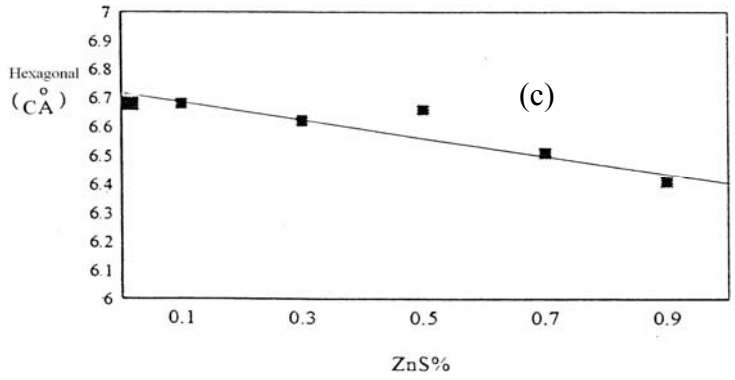

Fig. 11. Dependence of the lattice constant a and c of $Zn_xCd_{1-x}S$ films on zinc content (x).

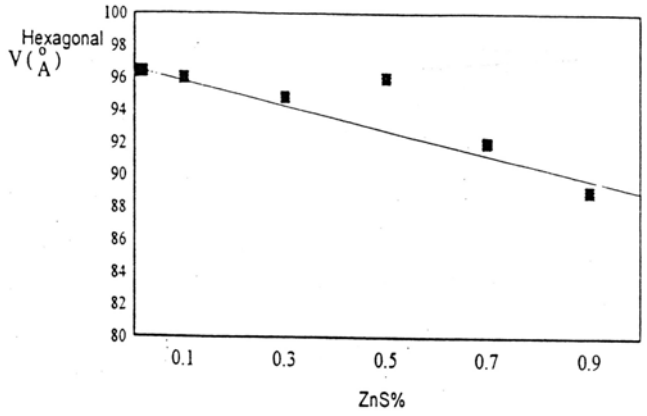

(a)

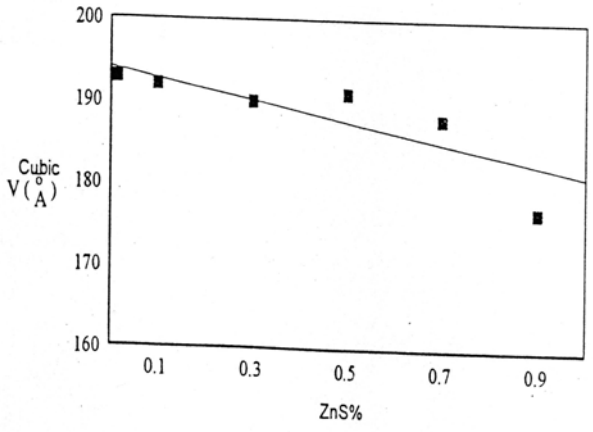

(b)

Fig. 12. Dependence of the volume of the unit cell V of $Zn_xCd_{1-x}S$ films on Zinc content (x).

4. Conclusion

$Zn_xCd_{1-x}S$ grown on glass substrates by (SGT) shows that the grown film is composed of mixture from both cubic and hexagonal structures. The present work reveals that, of the seven films the most homogenous films are those of $Zn_{0.5}Cd_{0.5}S$ films which is attributed to the graying nature of this film over the other films and the crystalline dimension of them film nears from the crystalline dimension of CdS film. X-ray diffraction study showed that the increase of Zn content in the film lead to all the peaks shifted towards the higher diffracting angles. The lattice constant also gradually decreased as Zn content increased. Optical study revealed that the

transmittance increases as Zn content increases. The strong absorption edge also shifted towards the lower wavelength region and hence the band gap of the films increases as Zn content increases.

However, CdS film is considered as the best of all these films because of its higher conductivity and because the band gap is widely used as a window material in heterojunction solar cells.

References

[1] L.E. Brus, J. Chem. Phys. **80**: 4403 (1984).
[2] N. C. Greenham, P. Xiaogang, A. P.Alivistos, Phys. Rev. **B54**: 1768 (1996).
[3] J. J. M. Halls, C.A. Walsh, N.C. Greenham, E.A. Marseglia, Nature **376**: 498 (1995).
[4] I. McClean, C. Thomas. Semicond. Sci. Technol. **7**, 1394 (1992).
[5] K. Yanta, K. Suzuki, Y. Oka, J. Appl. Phys. **73,** 4595 (1993).
[6] G. Yu, J. Gao, J.C. Hummeten, F. Wudl, A. J. Heeger, Science **270**, 1789 (1995).
[7] N. Karar, F. Singh, B.R. Mehta, J. Appl. Phys. 95, 656(2004).
[8] M. Morkel, L. Weinhardt, B. Lohmuller, C. Heske, E. Umbach, W. Riedl, S. Zweigart, F. Karg, Appl. Phys. Lett, 97: 4482 (2001)
[9] T. Yamaguchi, J. Matsufusa, A. Yoshida, Jpn. J. Appl. Phys. **31,** L703 (1992).
[10] T.Walter, M. Ruckh, K.O. Velthaus, H.W. Schock, in proceedings of the 11th Ec photovoltaic solar Energy conference Montreux p.124 (1992).
[11] G.K Padam, G.L. Malhotra and S.U.M. Rao, J. Appl. Phys. **63**(3), 770-774 (1988).
[12] L.C. Burton and T.L. Hench, Appl. Phs. Lett. **29**, 612 (1976).
[13] R.S. Feigelson, A. N. Diaye, S. Yin and R.H. Bube, J. Apple. Phys. **48**, 3162 (1977).
[14] D. Bonnet, Phys. States sold All: K 135 (1972).
[15] D.W. Ballentyne and B. Ray, Phsica. **27**, 337 (1961).
[16] H.L. Hwak, J. Phs. **D16**, 2367 (1983).
[17] G.K Padam, S.U. M. Rao and G.L. Malhotra, IEE Photovoltic specialists conference, vol. **II**: 1591 (1988).
[18] S. Jana, R. Maity, S.Das, M.K. Mitra, K.K. Chattopadhyay, Science Phys. **E39**; 109-114 (2007).
[19] M. Hetterich, S. Petillon, W. Petri, A. Dinger, M. Grün. Klingsh, J. Cryst. Grouth **159**:81 (1996).
[20] P. B. Smith, J. Vac. Sci. Technol. A **10** (4); 897-902 (1992).
[21] R.S. Feigelson, A. N'Diay, S.Y. Yin, R.H. Bube, J. Apple. Phys. **48** :3162 (1977).
[22] K.C. Park, H-B- Im, J. Electrochem. Soc: Solid State Science and Technology **135**, No. 4: 793-797 (1988).
[23] A.K. Atta, P.K. Biswats, D-Ganguli, Mater. Lett. **15**:99 (1992).
[24] B. Bhattacharjee, S.K. Modal, K. Chakrabarti, D. Ganguli, S. Chaudhuri, J. Phys. D.: Appl. Phys. **35,** 2636 (2002).
[25] L.C. Burton, T.L. Hench, Appl. Phys. Lett. No. 29:9 (1976).
[26] W.Palz, J. Besson, T. Ngujenduy, J. Vedel, Phaceedings of the 10th IEEE Photovoltaic specialists conference, palo Alto. Ca. (1973).
[27] W. Kane, J. Spratt, L. Hershinger, L. Kan, J. Electrochem. Soc. 113; 136 (1966).
[28] Y. Akdogan, C.Üzum, O. Dag, N. Coombs, J. Mater, Chem. 16:2048 (2006).
[29] I. Kaur, D.K. Pandya, K.L. Chopra, J. Electrochem. SOC: solid slate science and technology, vol. **127**, No. 4: 943 (1980).
[30] A. Mondal, T.K. Chaudhuri, P. Pramanik, Solar Energy Materials 7:431-438 (1983).
[31] D. Bonnet, Solar Cells, 11,21 (1984).
[32] N. Suyama, N. Ueno, K. Omura, H. Takada, Y. Kita, S. Kitamura, T. Hibino, M. Murozono; AU screen Printed $(CdZn)_s$/CdTe solar cell, (1987).
[33] M. Jayachandran, V.K. Venkatesan, T. Mahalingan, V. Vinni, Nanstructures and microstrcuture correlation with physical properties of semiconductor, Vol. **1284** : 260 (1990).
[34] C. Xing,, Y. Zhang, W. Yan, L. GUO Yaojunzhan, Weiyan, diegin C.Xing, Y. Zhan, W. Yan, L. Guo, Science International Journal of Hydrop Energy **31**: 2018-2024 (2006).